Knockdown of the E3 Ubiquitin ligase UBR5 and its role in skeletal muscle anabolism

Daniel C. Turner[1,2,3]*, David C. Hughes[4]*, Leslie M. Baehr[4]*, Robert A. Seaborne[3,5], Mark Viggars[3], Jonathan C. Jarvis[3], Piotr P. Gorski[1,2], Claire E. Stewart[3], Daniel J. Owens[3], Sue C. Bodine[4#] and Adam P. Sharples[1,2,3#]

[1]*Institute for Physical Performance, Norwegian School of Sport Sciences (NiH), Oslo, Norway*

[2]*Inst. for Science & Technology in Medicine (ISTM), School of Pharmacy and Bioengineering, Keele University, Staffordshire, UK*

[3]*Stem Cells, Ageing and Molecular Physiology Unit (SCAMP), Research Institute for Sport & Exercise Sciences (RISES), Liverpool John Moores University, Liverpool, UK*

[4]*Department of Internal Medicine, Division of Endocrinology and Metabolism, Carver College of Medicine, University of Iowa, Iowa City, IA, USA*

[5]*Centre for Genomics and Child Health, Blizard Institute, Barts and the London School of Medicine and Dentistry, Queen Mary University of London, UK*

* Primary Authors. These authors contributed equally to this work.

Corresponding authors

Corresponding Authors Details:

Sue C. Bodine & Adam P. Sharples

Email: sue-bodine@uiowa.edu & a.p.sharples@googlemail.com

Abstract

UBR5 is an E3-ubiquitin-ligase positively associated with anabolism, hypertrophy and recovery from atrophy in skeletal muscle. The precise mechanisms underpinning UBR5's role in the regulation of skeletal muscle mass remain unknown. The present study aimed to elucidate these mechanisms by silencing the UBR5 gene *in-vitro* and *in-vivo*. The siRNA-induced reduction (-77%) in UBR5 gene expression in human myotubes was prevented by mechanical loading, suggesting that UBR5 gene expression may be regulated via mechano-transduction signalling. Therefore, we electroporated a UBR5-RNAi plasmid into mouse tibialis anterior muscle *in-vivo* to investigate the impact of reduced UBR5 on mechano-transduction signalling MEK/ERK/p90RSK and Akt/p70S6K/4E-BP1/rpS6 pathways. Seven days post UBR5 RNAi electroporation, while reductions in overall muscle mass were not detected, mean CSA of GFP-positive fibers was reduced (-9.5%) and the number of large fibers was lower versus the control. Importantly, UBR5-RNAi significantly reduced total RNA, muscle protein synthesis, ERK1/2 and Akt phosphorylation. Whilst p90RSK phosphorylation significantly increased, total p90RSK protein levels demonstrated a 45% reduction with UBR5-RNAi. Finally, these early signalling events after 7 days of UBR5 knockdown culminated in significant reductions in muscle mass (-4.6%) and larger reductions in fiber CSA (-18.5%) after 30 days. This was associated with increased levels of the phosphatase, PP2Ac, and inappropriate chronic elevation of p70S6K and rpS6 between 7 and 30 days, and corresponding reductions in eIF4e. This study demonstrates UBR5 plays an important role in anabolism/hypertrophy, whereby knockdown of UBR5 culminates in skeletal muscle atrophy.

Running title: UBR5 knockdown and skeletal muscle anabolism

Keywords UBR5, siRNA, RNAi, Myotubes, Skeletal Muscle, Mechanical Loading, Hypertrophy, Electroporation, MAPK, ERK, p90RSK, Akt, P70S6K, rpS6, eIF4e, PP2Ac.

Introduction

The regulation of skeletal muscle (SkM) mass is orchestrated by the activity of key signalling pathways that control protein breakdown and synthesis within myofibers. The breakdown or atrophy of SkM mass is mediated, in-part, by the ubiquitin-proteasome system (3, 7), which is composed of three key enzymes that activate and conjugate (E1 & E2 enzymes) small ubiquitin molecules to target protein substrates (E3 ligases) for recognition and subsequent degradation in the 26S proteasome. The most characterised E3 ubiquitin ligases associated with SkM atrophy are the muscle specific RING finger protein 1 (MuRF1 or Trim63) and the F-box containing ubiquitin protein ligase atrogin-1 (Atrogin-1; Gomes *et al.*, 2001), otherwise known as muscle atrophy F-box (MAFbx; Bodine *et al.*, 2001*a*).

Interestingly, recent work identified that a HECT domain E3 ligase named, ubiquitin protein ligase E3 component n-recognin 5 (EDD1 or UBR5) was significantly altered at the DNA methylation and gene expression level following resistance exercise (RE) in human SkM (36, 37). UBR5 DNA methylation decreased (hypomethylated) and mRNA expression increased after 7 weeks of training-induced SkM hypertrophy, with further enhanced changes reported following a later 7 weeks of retraining (36, 37). The pattern observed in DNA methylation and gene expression, which significantly correlated with changes in lean mass, suggested that there may be a role for UBR5 during muscle hypertrophy in contrast to E3 ligases, MuRF1 and MAFbx that are associated with atrophy. Additional work has provided further support for this hypothesis, whereby UBR5 expression significantly increased after acute mechanical loading in bioengineered SkM *in-vitro*, in response to synergistic ablation/functional overload (FO), and after programmed resistance training in rodent muscle *in-vivo,* yet with no change in MuRF1 and MAFbx expression (35). UBR5 also increased during recovery from hindlimb unloading (HU) and tetrodotoxin induced-disuse atrophy, again with no increase in MuRF1 and MAFbx (35). Furthermore, increased gene expression of UBR5 in these models resulted in greater abundance of UBR5 protein content following FO-induced hypertrophy of the mouse plantaris muscle *in-vivo*, and over the time-course of regeneration in primary human muscle cells *in-vitro* (35). A recent study also supported the role of UBR5 as being essential for muscle growth through RNAi screening in *Drosophila* larvae, where UBR5 inhibition led to smaller sized larvae (23). Collectively, these data support the notion that UBR5 is involved in load-induced anabolism and hypertrophy, in contrast with the well-known MuRF1 and MAFbx E3 ligases that are associated with muscle atrophy.

33 The most characterised signalling pathway involved in anabolism, protein synthesis and
34 hypertrophy of SkM is the Akt/mTORC1/p70S6K pathway (Baar *et al.*, 2000; Bodine *et al.*, 2001;
35 Goodman *et al.*, 2011). Further work by the Esser laboratory also reported PI3K/Akt-independent
36 activation of mTORC via mitogen-activated protein kinase (MEK)/extracellular signal-regulated
37 kinase (ERK) signalling which was critical for overload-induced hypertrophy (28). Earlier work also
38 demonstrated increased ERK1/2 phosphorylation after acute resistance exercise (RE) in humans (13)
39 and after mechanical loading in C_2C_{12} myotubes (21). Downstream of ERK1/2, phosphorylation of
40 the ribosomal S6 kinase (p90RSK) has been shown to increase with acute endurance and resistance
41 exercise in rodent and human SkM (29, 43, 45). Interestingly, previous work also suggests that UBR5
42 is regulated via ERK/p90RSK signalling in non-muscle cells (9). Indeed, UBR5 has been shown to be
43 a target substrate for ERK2 in the COS-1 kidney fibroblast cell line after treatment with epidermal
44 growth factor (EGF), an established ligand that initiates downstream ERK signalling when bound to
45 its receptor (EGFR) (15). Others have also shown that p90RSK, phosphorylates UBR5 in HeLa cancer
46 cells at various sites, and may therefore be involved in growth of cancer cells (9). Further, UBR5 has
47 been suggested to target protein phosphatase 2A subunit C (PP2Ac; catalytic subunit) for
48 proteasomal degradation which is reported to negatively regulate Akt and ERK cascades (25–27,
49 38). Therefore, given that ERK/p90RSK signalling is associated with load-induced SkM hypertrophy
50 (28) and UBR5 is associated with ERK/p90RSK signalling in non-muscle cells (9, 15), assessing
51 ERK/p90S6K signalling as well as established load-induced Akt/ p70S6K signalling, together with
52 negative regulator PP2Ac, after experimental manipulation of UBR5 is required to elucidate UBR5s
53 mechanistic role in positively regulating muscle mass.
54
55 Therefore, in the present study, we first aimed to silence UBR5 (via siRNA) in human myotubes
56 during mechanical loading to understand UBR5s role in response to loading. We demonstrated that
57 siRNA-induced silencing of UBR5 in non-loaded control conditions reduced its gene expression by
58 ~77%, and that this reduction in expression was completely prevented by the addition of mechanical
59 loading. Providing positive evidence towards our hypothesis that UBR5 gene expression was
60 perhaps regulated via mechano-transduction signalling. Therefore, to test this hypothesis we used
61 a miR-based RNAi for UBR5, using pcDNA TM 6.2-GW/EmGFP-miR electroporated into murine
62 tibialis anterior (TA) muscle, to investigate the impact of reduced UBR5 on MEK/ERK/p90RSK/MSK1
63 and PP2Ac/Akt/GSK3β/p70s6K/rpS6/eIF4e signalling *in-vivo*. UBR5 silencing led to a reduction in the
64 CSA of transfected fibers, the frequency of larger fibers (≥3400 μm^2), total RNA content, protein
65 synthesis, ERK1/2 and Akt activity and total p90RSK levels. However, activity of p90RSK, p70S6K and

66 rpS6 activity increased. Finally, the changes at 7 days also culminated in even larger reductions in
67 muscle mass and fiber CSA after 30 days post transfection of UBR5 RNAi. This was also associated
68 with increased PP2Ac and chronic elevation of p70S6K and rpS6 between 7 and 30 days, as well as
69 reductions in eIF4e. Overall, the present study supports the notion that UBR5 plays an important
70 role in muscle anabolism/hypertrophy, and that a reduction in UBR5 is associated with early
71 reductions in ERK1/2, Akt activity, total p90RSK and protein synthesis that culminates in later
72 atrophy via increased PP2Ac and inappropriate activation of p70S6K and rpS6 signaling.
73
74 **Methods**
75 *Skeletal Muscle Tissue and Ethical Approval*
76 Prior to collection of human skeletal muscle (SkM) tissue, participants gave written informed
77 consent. Ethical approval was granted by the NHS West Midlands Black Country, UK, Research Ethics
78 Committee (NREC approval no. 16/WM/0103). Muscle tissue was handled and stored in accordance
79 with Human Tissue Act (2004) regulations. For *in-vitro* myotube experiments, human SkM biopsies
80 were obtained from the vastus lateralis muscle of young healthy males (23 ± 3.2 yrs, 75.4 ± 3.7 kg,
81 180.7 ± 2.1 cm, BMI 23.1 ± 1.5 kg/m^2) using a needle biopsy instrument (CR Bard, Crawley, UK) as
82 described fully elsewhere (Turner *et al.*, 2019*a*). For *in-vivo* muscle tissue experiments, C57Bl/6 male
83 mice between twelve and sixteen weeks-old (*n* = 10) were obtained from Charles River Laboratories
84 for electroporation experiments. All animal procedures were approved by the Institutional Animal
85 Care and Use Committee at the University of Iowa. During tissue collection, animals were
86 anaesthetized with 2–3% inhaled isoflurane. On completion of tissue removal, mice were
87 euthanised by exsanguination.
88
89 *Isolation and Culture of Human Skeletal Muscle Derived Cells (HMDC)*
90 Following human biopsy procedures, muscle tissue was placed in sterile microfuge tubes (Ambion®,
91 Thermo Fisher Scientific Denmark) containing 1.5 ml of chilled (4˚C) transfer media composed of
92 Ham's F-10 medium including 1 mM L-glutamine (LG; Thermo Fisher Scientific, Denmark), 0.1% heat
93 inactivated fetal bovine serum (hiFBS; Gibco™, South America Origin, Fisher Scientific, UK), 0.1% heat
94 inactivated new born calf serum (hiNBCS; Gibco, New Zealand Origin, Fisher Scientific, UK), 100 U/ml
95 penicillin (Lonza, UK), 100 µg/ml streptomycin (Lonza, UK), 2.5 µg/ml amphotericin B (Sigma-Aldrich,
96 UK) and transported on ice to a class II biological safety cabinet (Kojair Biowizard Silverline, Finland)
97 to undergo subsequent cell isolations as described in previous work by our group (10, 32, 40).
98 Briefly, muscle tissue was minced in 5 ml trypsin (0.05%)/EDTA (0.02%) solution using 2 × sterile

99 scalpels (No. 11, Swann-Morton, UK). The contents were transferred to a sterile specimen pot and
100 magnetically stirred at 37˚C for 10 mins. This process was repeated, and then homogenised tissue
101 was placed in a sterile 15 ml tube (Falcon®, Fisher Scientific, UK) containing 2 ml heat inactivated
102 horse serum (hiHS; Gibco™, New Zealand Origin, Fisher Scientific, UK) to neutralise the trypsin. The
103 tube was centrifuged (340 × g for 5 min at 24˚C) and the supernatant was seeded on to 2 separate
104 pre-gelatinised (0.2% in dH_2O; Type A, Sigma-Aldrich, UK) T25 flasks (Nunc™, Thermo Fisher
105 Scientific, Denmark) containing 7.5 ml of growth medium (GM, composed of Ham's F-10 medium
106 that included 1 mM LG, 10% hiFBS, 10% hiNBCS, 4 mM LG, 100 U/ml penicillin, 100 µg/ml
107 streptomycin and 2.5 µg/ml amphotericin B). All flasks were then incubated (HERAcell 150i CO_2
108 humidified incubator, Thermo Fisher Scientific, Denmark) at 37˚C and 5% CO_2 until ~80% confluency
109 was attained. Cells were then transferred to T75 flasks and passaged (P7-9) until sufficient cell
110 quantities were acquired for experimentation.
111
112 *Immunocytochemistry for Desmin Positivity of HDMC*
113 HMDC were washed 3 × TBS (1×; Sigma-Aldrich, UK) and fixed in ice-cold methanol:acetone:TBS
114 (25:25:50 for 15 mins) then in methanol:acetone (50:50) for a further 15 mins. Following fixation,
115 HMDC were permeabilised in 0.2% Triton X-100 (Sigma-Aldrich, UK) and blocked in 5% goat serum
116 (Sigma-Aldrich, UK) in TBS for 90 mins. Cells were washed 3 × in TBS and incubated overnight (4˚C)
117 in 300 µl of anti-desmin (Abcam Cat# ab15200, RRID: AB_301744) primary antibody made up in TBS,
118 2% goat serum and 0.2% Triton X-100 at concentrations of 1:50. After overnight incubation, the
119 primary antibody was removed and HMDC were washed 3 × in TBS. Cells were incubated at RT for
120 3 hrs in 300 µl secondary antibody solution containing anti-rabbit TRITC (Sigma-Aldrich Cat# T6778,
121 RRID: AB_261740) at a concentration of 1:75 in 1× TBS, 2% goat serum and 0.2% Triton X-100 to
122 counterstain myoblasts. After a further 3 × TBS washes, 300 µl of DAPI (Thermo Fisher Scientific Cat#
123 D1306, RRID: AB_2629482) was added to the cells at a concentration of 300 nM for 30 mins to
124 counterstain myonuclei. Immunostained HMDC were visualised and imaged using confocal
125 microscopy (Olympus IX83, Japan) with TRITC (Excitation: 557 nm, Emission: 576 nm) and DAPI
126 (Excitation: 358 nm, Emission: 461 nm) filter cubes. Immuno-images were imported to Fiji/ImageJ
127 (version 2.0.0) software to determine desmin positivity via counting the total number of myoblasts
128 overlapping nuclei divided by the total number of nuclei present. Desmin positivity was the same
129 across all participants (72 ± 2.4%).
130
131

132 *Transfection of UBR5 siRNA into Human Myotubes*

133 After serial passaging, HMDC (passage 7-9) were seeded onto plastic 6-well fibronectin-coated (10
134 µg/ml in PBS, Sigma-Aldrich, UK) culture plates (described below) at a density of 9×10^4 cells/ml in
135 2 ml GM. Once 80% confluency was attained, medium was switched to 2 ml differentiation media
136 (DM; same media components as GM with the exception of lower 2% hiFBS) for the remaining 10
137 days. Each well received an additional 1 ml of DM at 72 hrs and 7 days. At day 10, existing media
138 was removed and the resulting myotubes received either 750 µl of fresh DM alone or 750 µl DM
139 containing 9 µl HiPerFectTransfection™ (Qiagen, UK) and 20 nmol Flexitube GeneSolutions™ (siUBR5,
140 Qiagen, UK). The Flexitube GeneSolutions includes 4 × siRNA's that target multiple regions of the
141 10900 bp UBR5/EDD1 human gene (see figure in results) and evoked a 77 ± 1.28% (mean ± SEM)
142 reduction in UBR5 gene expression after 3 hours when using a 20 nmol concentration. All siRNA
143 target sequences and locations are displayed in the results figures. Also, using a scramble siRNA
144 (Qiagen, AllStars Negative Control siRNA™ including HiPerFectTransfection reagent) we confirm that
145 we saw no significant reduction in UBR5 at this 3h time point. Please note that we first established
146 the recommended 10 nmol siRNA concentration did not reduce UBR5 gene expression substantially
147 (reduction of only 25.72 ± 4.72%) in human myotubes and that higher concentrations were
148 therefore required during loading experiments.

149

150 *Mechanical Loading of Myotubes*

151 HMDC were first differentiated on fibronectin-coated (10 µg/ml in PBS, Sigma-Aldrich, UK) flexible-
152 bottomed culture plates (25 mm BioFlex®, Dunn Labortecknik, Germany) for 10 days as described
153 above. Resultant myotubes were dosed with either 20 nmol UBR5 siRNA or DM alone, immediately
154 after which, loading experiments commenced. Myotubes were subjected to equibiaxial tension
155 using the Flexcell® FX-5000™ Tension system (Dunn Labortecknik, Germany) and a low frequency
156 (0.15 Hz with sine wave) intermittent loading regime was applied. The loading regime consisted of
157 4 sets × 10 repetitions with 90 s rest between sets, representing 1 loading session. This was repeated
158 5 times with each loading session interspersed with a 3.5 min rest, totalling a regime of 60 mins.
159 Non-loaded control myotubes were also assembled to the Flexcell® base plate, however, the vacuum
160 entry was sealed to avoid any unwanted loading. Following cessation of mechanical loading, both
161 loaded and non-loaded myotubes were lysed for RNA at 3 hrs. Due to the low number of human
162 cells available for these experiments, protein extraction for signalling analysis was not possible.

163

164

165 *RNA Extraction, Primer Design and Polymerase Chain Reaction (PCR) (Human myotubes)*

166 After incubation, existing media was removed and myotubes were washed 2 × in PBS before lysing
167 cells with 300 µl TRIzol (Invitrogen™, Thermo Fisher Scientific, Denmark) for subsequent RNA
168 extraction. RNA concentrations and purities (i.e. A_{260}/A_{280} ratios) were quantified using a
169 spectrophotometer (NanoDrop™ 2000, Thermo Fisher Scientific, Denmark). A_{260}/A_{280} ratios
170 demonstrated high quality RNA across all samples (1.91 ± 0.22, mean ± SD). A one-step PCR kit
171 (QuantiFast™ SYBR® Green, Qiagen, UK) was used to assess gene expression. Firstly, samples were
172 diluted in nuclease-free H_2O to ensure a concentration of 35 ng RNA in 10 µl reactions, made up of:
173 4.75 µl (7.37 ng/µl) RNA sample and 5.25 µl of master mix (MM) composed of 5 µl SYBR green mix,
174 0.1 µl of reverse transcriptase (RT) mix and 0.075 µl of both forward and reverse primers (both at
175 100 µM). Primers were designed using both Clustal Omega
176 (https://www.ebi.ac.uk/Tools/msa/clustalo/) and Primer-BLAST (NCBI,
177 https://www.ncbi.nlm.nih.gov/tools/primer-blast/) and were purchased from Sigma-Aldrich. All
178 primer sequence information is described in Table 1. PCR reactions were transferred to a qRT-PCR
179 thermocycler (Rotorgene 3000Q, Qiagen, UK) with supporting software (Hercules, CA, USA) to
180 undergo amplification as follows: 10 min hold at 50˚C (reverse transcription/cDNA synthesis), 95˚C
181 for 5 min (transcriptase inactivation and initial denaturation step) and PCR Steps of 40 cycles; 95˚C
182 for 10 s (denaturation), 60˚C for 30 s (annealing and extension). Upon completion, melt curve
183 analyses was carried out to identify non-specific amplification or primer-dimer issues for the
184 reference genes (B2M and RPL13a) and UBR5. These analyses demonstrated a single melt
185 curve/peak for all genes. Gene expression was then quantified using the DDCT ($2^{-\Delta\Delta CT}$) equation
186 (33) against the mean of 2 reference genes (B2M and RPL13a, 15.33 ± 0.7 with low variation across
187 all conditions of 4.56%) and the mean C_T value derived from the non-treated DM group for each
188 time point (0/3 hrs) and condition (non-loaded/loaded). The PCR efficiencies were similar for the
189 reference genes, RPL13a (97.4 ± 7.75%, with 7.96% variation) and B2M (92.08 ± 3.18%, with 3.46%
190 variation), and the gene of interest, UBR5 (90.93 ± 4.94%, with 5.43% variation).

191

192

193

194

195

196

197

198 **Table 1.** Primer sequence information for genes analysed in human myotubes.

Target Gene	Primer Sequence (5'-3')	Product Length (bp)
UBR5	F: AGGCAACACCTTAGGAAGC	81
	R: GCTCCAGCTGATGACCTAC	
RPL13a	F: GGCTAAACAGGTACTGCTGGG	104
	R: GGAAAGCCAGGTACTTCAACTT	
B2M	F: CCGTGTGAACCATGTGACT	91
	R: TGCGGCATCTTCAAACCT	

199

200 *Plasmid Design and Electroporation of Tissue In-Vivo*

201 An RNAi system which was designed and purchased from Invitrogen (Thermo Fisher Scientific, *USA*)
202 was implemented. Specifically, the negative control/empty vector (EV) RNAi plasmid was described
203 previously (14, 22, 35) and encodes emerald green fluorescent protein (EmGFP) and a non-targeting
204 pre-miRNA under bicistronic control of the CMV promoter in the pcDNA6.2GW/EmGFP-miR plasmid
205 (Invitrogen). The UBR5 RNAi plasmid also encodes EmGFP plus an artificial pre-miRNA targeting
206 mouse UBR5 under bicistronic control of the CMV promoter. It was generated by ligating the
207 Mmi571982 oligonucleotide duplex (Invitrogen) into the pcDNA6.2GW/EmGFP-miR plasmid. The
208 UBR5 RNAi plasmid is designed to target the nucleotide sequence in the HECT domain between
209 amino acids positions 2695-2754 (location/schematic of the RNAi on UBR5 protein structure is also
210 included in the results). The electroporation technique was performed as previously described (35).
211 Briefly, after a 2hr pre-treatment with 0.4 units/ul of hyaluronidase, 20 µg plasmid DNA was injected
212 into the tibialis anterior (TA) muscle and the hind limbs were placed between two-paddle electrodes
213 and subjected to 10 pulses (20 msec) of 175 V/cm using an ECM-830 electroporator (BTX Harvard
214 Apparatus). Mice were injected with the UBR5 RNAi plasmid and an empty vector (EV) control into
215 the contralateral muscle. TA muscles were harvested after 7 and 30 days.

216

217 *Mouse Skeletal Muscle Tissue Collection*

218 Following completion of the appropriate time period, mice were anesthetized with isoflurane, and
219 the TA muscles were excised, weighed, frozen in liquid nitrogen, and stored at −80°C for later
220 analyses. Muscles were collected for histology (n = 5) and RNA/Protein isolation (n = 5) and
221 processed as described below. On completion of tissue removal, mice were euthanized by
222 exsanguination.

223

224 *Immunohistochemistry and Histology Tissue*

225 Harvested mouse TA muscles were immediately weighed and fixed in 4% (w/v) paraformaldehyde
226 for 16 h at 4˚C and then placed in 30% sucrose for overnight incubation. The TA muscles were then
227 embedded in Tissue Freezing Medium (Triangle Biomedical Sciences), and a Thermo HM525 cryostat
228 was used to prepare 10 µm sections from the muscle mid-belly. All sections were examined and
229 photographed using a Nikon Eclipse Ti automated inverted microscope equipped with NIS-Elements
230 BR digital imaging software.

231

232 *Laminin Stain of Tissue*

233 TA muscle sections were permeabilized in PBS with 1% triton for 10 minutes at room temperature.
234 After washing with PBS, sections were blocked with 5% goat serum for 15 minutes at room
235 temperature. Sections were incubated with Anti-Laminin (1:500, Sigma-Aldrich Cat# L9393, RRID:
236 AB_477163) in 5% goat serum for 2 hours at room temperature, followed by two 5-minute washes
237 with PBS. Goat-anti-rabbit AlexaFluor® 555 secondary (1:333, Invitrogen Cat# A28180, RRID:
238 AB_2536164) in 5% goat serum was then added for 1 hour at room temperature. Slides were cover
239 slipped using ProLong Gold Antifade reagent (Life Technologies). Image analysis was performed
240 using Myovision software (41). Skeletal muscle fiber size was analyzed by measuring ≥ 250
241 transfected muscle fibers per muscle, per animal (10x magnification). Transfected muscle fibers
242 were identified as GFP-positive as shown in results figures for 7 days and 30 days. We also measured
243 the size of non-transfected fibers (GFP-negative) from the transfected muscles at all time points.
244 Comparison of the CSA distributions of GFP-negative fibers in EV and UBR5 RNAi transfected
245 muscles revealed no difference between groups. Therefore, fiber size comparisons were made
246 between the GFP-positive fibers in the EV controls and UBR5 RNAi transected muscles.

247

248 *RNA Isolation and Total RNA Quantification of Tissue*

249 Prior to RNA isolation, aliquots of frozen muscle powder were weighed in order to calculate RNA
250 per milligram of wet muscle tissue. Muscle powder was homogenized using RNAzol RT reagent
251 (Sigma-Aldrich, St Louis, MO) in accordance with the manufacturer's instructions. Total RNA
252 quantity and quality was assessed for 260/280 ratios using a SpectraMax M2 Microplate reader
253 (Molecular Devices, CA, USA).

254

255

256

257 *Muscle Protein Synthesis (MPS) in Tissue*

258 Changes in MPS were assessed in TA muscles transfected for 7 days by measuring the incorporation
259 of exogenous puromycin into nascent peptides as described previously (19, 42). Puromycin (EMD
260 Millipore, Billerica, MA, USA; cat. no. 540222) was dissolved in sterile saline and delivered
261 (0.02 µmol g^{-1} body weight by I.P. injection) 30 min prior to muscle collection.

262

263 *Immunoblotting in Tissue Lysates*

264 Frozen TA muscles were homogenized in sucrose lysis buffer (50 mM Tris pH 7.5, 250 mM sucrose,
265 1 mM EDTA, 1 mM EGTA, 1% Triton X 100, 50 mM NaF). The supernatant was collected following
266 centrifugation at 8,000 *g* for 10 minutes and protein concentrations were determined using the 660-
267 protein assay (Thermo Fisher Scientific, Waltham, MA). Twelve micrograms of protein were
268 subjected to SDS-PAGE on 4-20% Criterion TGX stain-free gels (Bio-Rad, Hercules, CA) and
269 transferred to polyvinylidene diflouride membranes (PVDF, Millipore, Burlington, MA). Membranes
270 were blocked in 3% nonfat milk in Tris-buffered saline with 0.1% Tween-20 added for one hour and
271 then probed with primary antibody (concentrations detailed below) overnight at 4°C. Membranes
272 were washed and incubated with HRP-conjugated secondary antibodies at 1:10,000 (Mouse, Cell
273 Signaling technology Cat# 7076, RRID AB_330924; Rabbit, Cell Signaling technology Cat# 7074, RRID
274 AB_2099233) for one hour at room temperature. Immobilon Western Chemiluminescent HRP
275 substrate was then applied to the membranes prior to image acquisition. Image acquisition and
276 band quantification were performed using the Azure C400 System (Azure Biosystems, Dublin, CA,
277 USA) and Image Lab, version 6.0.1 (Bio-Rad), respectively. Total protein loading of the membranes
278 captured from images using stain-free gel technology was used as the normalization control for all
279 blots. The following primary antibodies were used all used at a concentration of 1:1000: Cell
280 Signaling Technologies (Danvers, MA, USA) – phospho-ERK1/2 $^{Thr202/Tyr204}$ (Cat# 4370,
281 RRID:AB_2315112), ERK1/2 (Cat# 4695, RRID:AB_390779), phospho-p90RSK ^{Ser380} (Cat# 11989,
282 RRID:AB_2687613), p90RSK (Cat# 9355, RRID:AB_659900), phospho-MSK1 ^{Thr581} (Cat# 9595,
283 RRID:AB_2181783), phospho-MEK1/2 $^{Ser217/221}$ (Cat# 9154, RRID:AB_2138017), phospho-Akt ^{Ser473}
284 (Cat# 4060, RRID:AB_2315049), Akt (Cat# 9272, RRID:AB_329827), phospho-GSK3β ^{Ser9} (cat. Cat#
285 9336, RRID:AB_331405), GSK3β (Cat# 9332, RRID:AB_2335664), phospho-p70S6K Thr^{389} (Cat# 9205,
286 RRID:AB_330944), p70S6K (Cat# 9202, RRID:AB_331676), phospho-rpS6 $^{Ser240/244}$ (Cat# 5364,
287 RRID:AB_10694233), rpS6 (Cat# 2217, RRID:AB_331355), phospho-4EBP1 $^{Thr37/46}$ (Cat# 2855, RRID:
288 AB_560835), 4EBP1 (Cat# 9644, RRID:AB_2097841) UBR5 (Cat# 65344, RRID:AB_2799679), PP2Ac
289 (Cat# 2259, RRID:AB_561239), eIF4e (Cat# 9742, RRID:AB_823488) and EMD Millipore – puromycin

290 (Cat# MABE343, RRID:AB_2566826). Knockdown of UBR5 protein was confirmed previously with a
291 reduction of 60% (Seaborne *et al.*, 2019) and all signaling antibodies in the present study were
292 processed on the same samples as this UBR5 protein data.
293
294 *Statistical Analysis*
295 Paired student *t-tests* were first carried out to assess knockdown efficiency (%) in siUBR5 treated
296 vs. DM non-treated cells at in loaded and non-loaded myotubes. Also, to determine UBR5 mRNA
297 fold-change in loaded vs. non-loaded myotubes dosed with DM alone. Finally, paired *t-tests* were
298 carried out when comparing empty control (EV) vs. UBR5 RNAi transfected mouse TA SkM. All
299 statistical analysis was performed using GraphPad Software (Prism, Version 7.0a, San Diego, CA).
300 Data is presented as mean ± standard error of the mean (SEM). $P \leq 0.05$ represents statistical
301 significance.
302
303 **Results**
304 *siRNA induced reductions in UBR5 gene expression are prevented with mechanical loading*
305 We first wished to determine the impact of UBR5 silencing and mechanical loading on UBR5 gene
306 expression in human myotubes (Figure 1A-F). There was an increase in mean UBR5 gene expression
307 at 3 hrs post-loading in DM control conditions (158 ± 54.5% / ~1.58-fold increase, Figure 1G),
308 however this did not quite reach statistical significance. Following 3 hrs of UBR5 siRNA treatment
309 (Figure 1H) in non-loaded myotubes, there was a significant decrease in UBR5 gene expression (-77
310 ± 1.28% $P < 0.001$; Figure 1G). Importantly, gene silencing of UBR5 at 3 hrs was prevented by
311 mechanical loading, demonstrated by a return to baseline levels of UBR5 expression (Figure 1G) in
312 the siUBR5 + loading condition (Figure 1G).
313

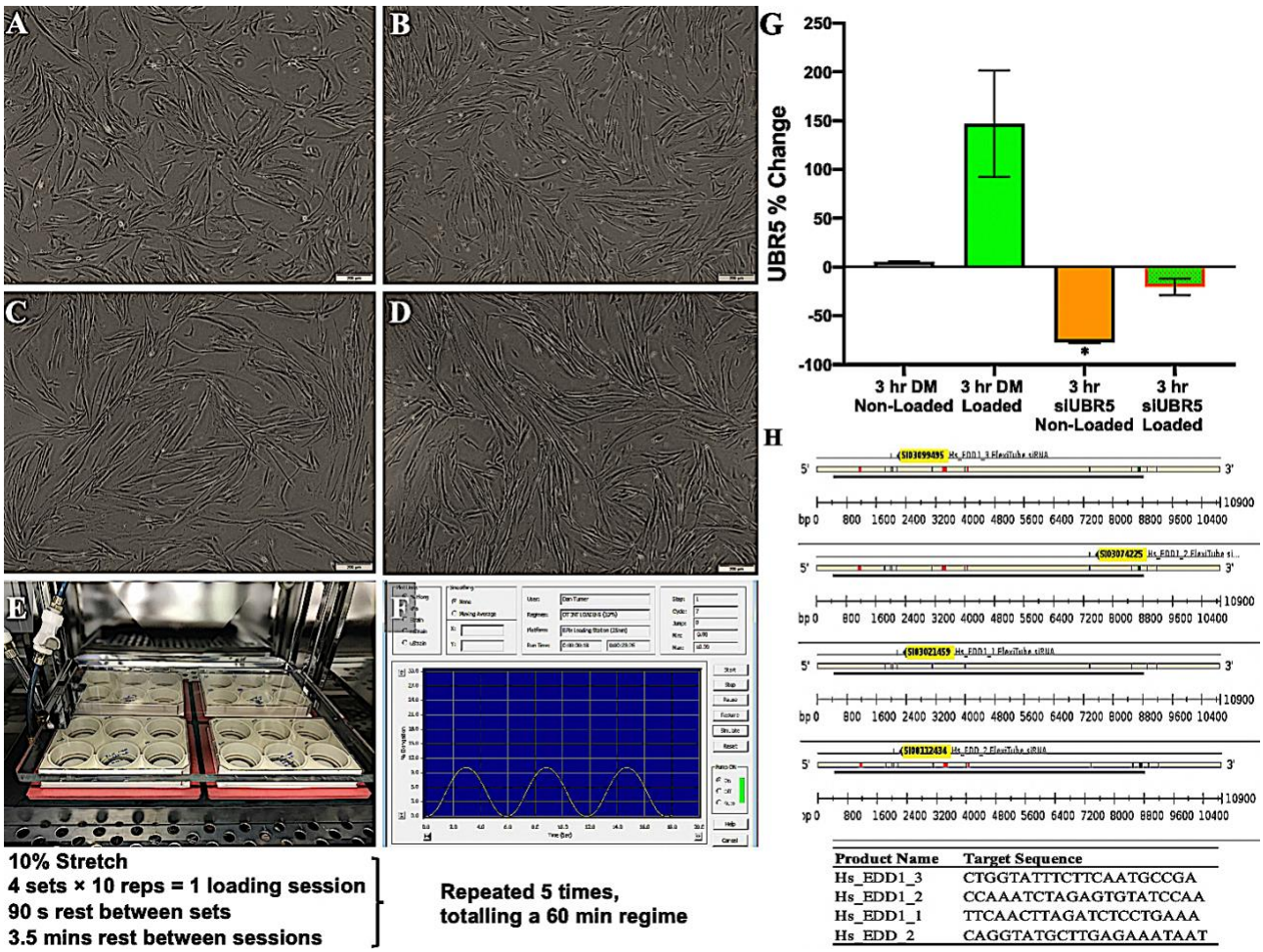

Figure 1. UBR5 gene silencing and mechanical loading of human myotubes. Cultured HMDC at **(A)** 0 hrs, **(B)** 72 hrs, **(C)** 7 days and **(D)** 10 days in DM (10× magnification, Olympus, CKX31) **(E)** HMDC cultured/differentiated into myotubes at day 10 and mechanically loaded on BioFlex® well plates using Flexcell® technology within a humidified incubator at 37˚C/5 Co_2%. **(F)** Example of the sine wave profile during the mechanical loading regime. **(G)** UBR5 gene expression increases (158 ± 54.6%) in loaded versus non-loaded myotubes. Silencing of UBR5 using siRNA reduced UBR5 mRNA expression (~77%) in human myotubes after 3 hours. Mechanical loading prevented the reduction in UBR5 gene expression in UBR5 siRNA conditions back towards baseline levels at 3 hrs post-loading. **(H)** Graphical representation of the 4 × siRNA's (siUBR5) used, and the sequence locations on the EDD1/UBR5 human gene (NM_015902, 10900 bp length). (*) Depicts statistical significance ($P \leq 0.05$). Data is present as mean ± standard error of mean (SEM).

Fiber CSA was significantly reduced at 7 days post electroporation in mice

To examine the effect of reducing UBR5 expression *in-vivo*, mouse TA muscles were transfected with either UBR5 RNAi plasmid targeting UBR5s HECT domain (Figure 2A) or an EV control. UBR5 protein was significantly reduced by 65% (± 11.8%) in UBR5 RNAi conditions (Figure 2B), as previously demonstrated in (35). The TA mass (mg) did not significantly change at 7 days post electroporation in UBR5 RNAi vs. EV transfected TA muscle (Figure 2C). Interestingly, however, measurement of the CSA of GFP-positive fibers revealed that the mean fiber CSA of GFP-positive

333 fibers was significantly reduced (-9.5 ± 3.2%) in RNAi transfected TA muscle (*P* = 0.048; Figure 2D &
334 E) with fewer larger fibers (≥3400 µm^2) present versus the EV (Figure 2D & F).

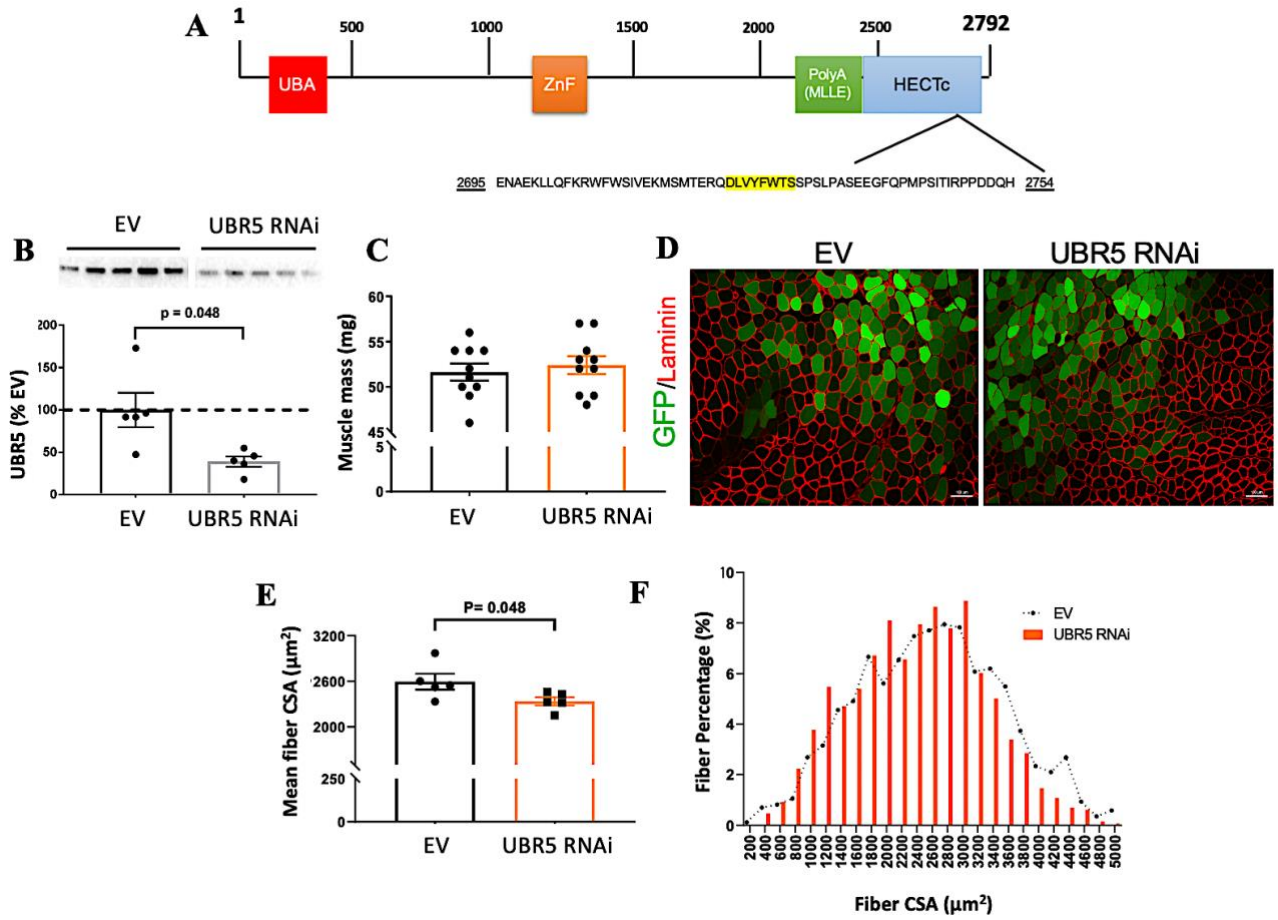

335

336 **Figure 2. Characteristics of tibialis anterior muscle mass and fiber CSA in UBR5 RNAi transfected TA muscle after 7**
337 **days. (A)** Schematic/ putative domain structure of UBR5 protein consisting of ubiquitin-associated (UBA) domain-like
338 superfamily, Putative zinc finger in N-recognin (ZnF), Poly-adenylate binding protein (PolyA), MLLE protein/protein
339 interaction domain and a HECT domain. The UBR5 RNAi plasmid was designed to target the nucleotide sequence in the
340 HECT domain between amino acids position 2695-2754 (highlighted in yellow in A). **(B)** TA skeletal muscles were
341 transfected for 7 days and we confirmed that the RNAi plasmid significantly reduced UBR5 protein levels by 65%
342 (Seaborne et al., 2019) in basal mouse skeletal muscle. We have previously confirmed significant reductions in UBR5
343 protein levels at 7 days with this UBR5 RNAi plasmid (Seaborne et al., 2019) , and all 7 day data in the present manuscript
344 (muscle mass (C), histology (D), fiber CSA (E) RNA and signalling data – figure below) is analyzed from the same
345 animals/samples as this UBR5 protein data. Figure 2B is therefore reused with permissions from; R. A. Seaborne et al.,
346 *Journal of Physiology* (Wiley), 597.14 (2019) pp 3727–3749, Copyright-2019 The Authors. *The Journal of Physiology*.
347 Copyright-2019 The Physiological Society). **(C)** After 7 days, muscle mass was no different between empty vector control
348 (EV) and UBR5 RNAi transfected TA muscles (*n* = 10 per group). **(D)** Representative images (10x magnification; scale bar
349 = 100 µm) for GFP transfected fiber identification and CSA quantification through Laminin staining. **(E)** A significant
350 reduction (*P* = 0.05) in mean transfected fiber CSA size was observed in the RNAi transfected vs. EV muscles *(n* = 5 per
351 group). **(F)** Quantification of muscle CSA revealed changes in the percentage of small fibers (<1200 µm^2) and large fibers
352 (≥3400 µm^2) with RNAi transfected muscles verses EV group (N = 5 per group). Data presented as Mean ± SEM. Statistical
353 significance is depicted where present (P ≥ 0.05).

354 *Total RNA concentrations, muscle protein synthesis, ERK1/2 and Akt activity and total p90RSK are*
355 *reduced in UBR5 RNAi TA muscle after 7 days*
356 Along with a reduction in fiber CSA at 7 days post UBR5 RNAi, a significant reduction in total RNA
357 concentrations (*P* = 0.01, Figure 3A) and protein synthesis (-17 ± 3.2%, *P* = 0.05, Figure 3B & 3C) was
358 evident. Wishing to determine potential regulators of this process in the ERK signalling pathway
359 (Figure 3D), ERK1/2 (p44/42 MAPK) was examined and found to be reduced (-43 ± 2.3%, *P* = 0.03,
360 Figure 3E). Interestingly, the reduction in RNA, protein synthesis and ERK1/2 signalling coincided
361 with a significant increase in phospho-p90RSK^{Ser380} (170 ± 39.8%, *P* = 0.04; Figure 3F) at 7 days.
362 However, this was on the background of a significant 45% decrease in total p90RSK (-45 ± 5.6%, P =
363 0.02; Figure 3G) with no significant change in total ERK1/2 protein levels were observed in UBR5
364 RNAi transfected muscles. We also observed no differences in the phosphorylation of MEK 1/2^{Ser}
365 $^{217/221}$ or MSK-1^{Thr581} between RNAi and EV transfected TA muscles after 7 days (data not depicted).
366 We next assessed protein signalling associated with the Akt pathway (Figure 4A). As with ERK1/2,
367 there were significant reductions in Akt ^{ser473} phosphorylation in UBR5 RNAi transfected TA muscle
368 (-26 ± 9%, P = 0.03; Figure 4B), with no differences in GSK-3β ^{Ser9} phosphorylation after 7 days post-
369 electroporation (Figure 4A). Interestingly, despite reductions in ERK1/2, Akt and protein synthesis,
370 we observed significant elevations in phosphorylation for p70S6K ^{Thr389} (176 ± 57%, P = 0.02; Figure
371 4C) and rpS6 $^{Ser240/244}$ (178 ± 39.4%, P = 0.01; Figure 4D) in UBR5 RNAi transfected muscles at 7 days.
372 Finally, there were no changes in activity of 4E-BP1 $^{Thr37/46}$, eiF4e or PP2Ac at 7 days in UBR5 RNAi
373 transfected muscles (Figure 4A).

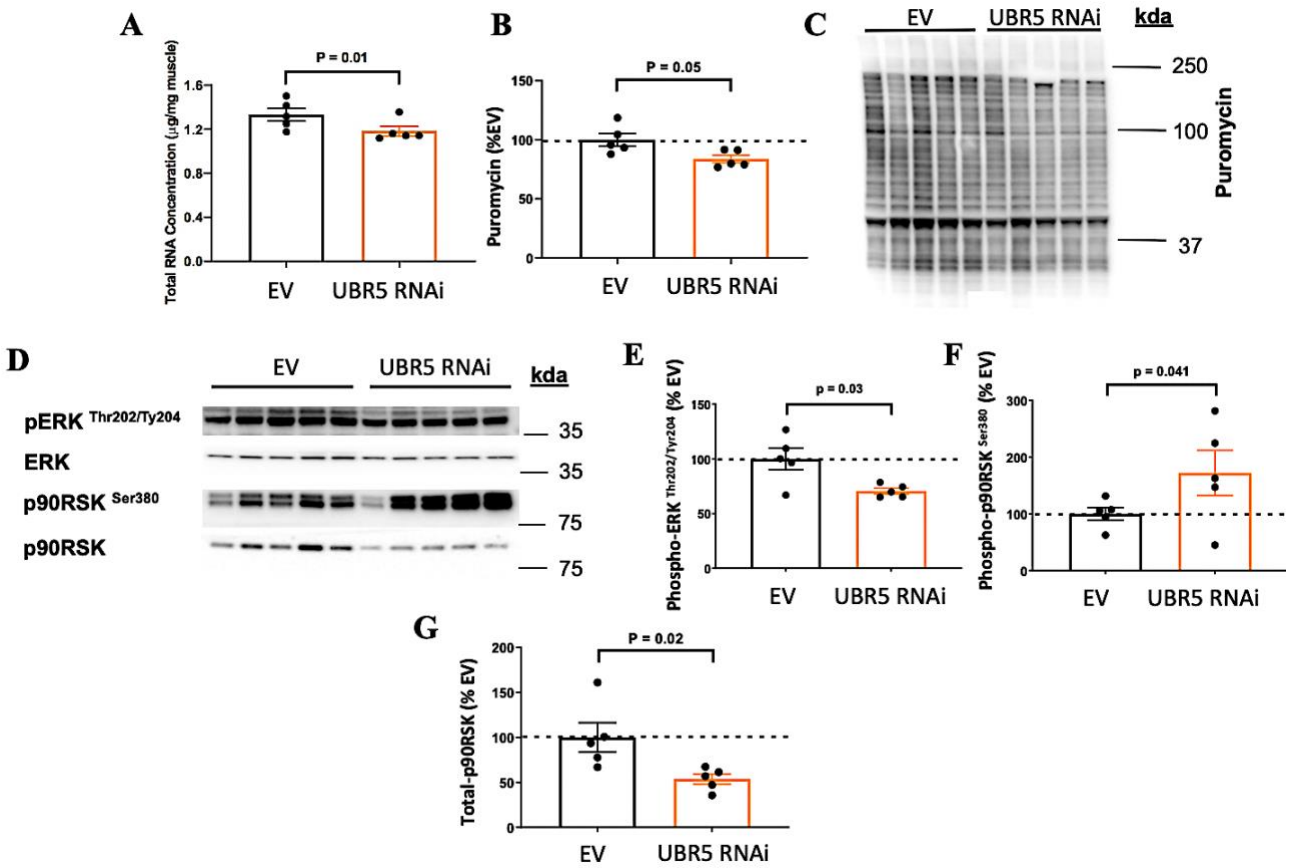

Figure 3. Alteration in total RNA, protein synthesis and MAPK (ERK/p90RSK) signaling in UBR5 RNAi transfected TA muscle after 7 days. (A) Total RNA concentration (assessed as µg/mg of muscle) was significantly reduced (*P* = 0.01) in the UBR5 RNAi muscles. **(B & C)** RNAi transfected muscles also displayed a significant reduction (~17%, *P* = 0.05) in muscle protein synthesis (B) assessed via western blots for puromycin incorporation (C). **(D)** Western blot images for the ERK signaling pathway. **(E)** Decreased phosphorylation levels of ERK1/2 (p44/42 MAPK) *(P* = 0.03) and **(F)** increased phosphorylation levels of p90RSK (*P* = 0.04) with UBR5 RNAi. **(G)** Reduced levels of total p90RSK (*P* = 0.02). Data presented as Mean ± SEM. Total protein loading of the membranes captured from images using stain-free gel technology was used as the normalization control for all blots. N = 5 per group. Statistical significance is depicted where present (P ≥ 0.05).

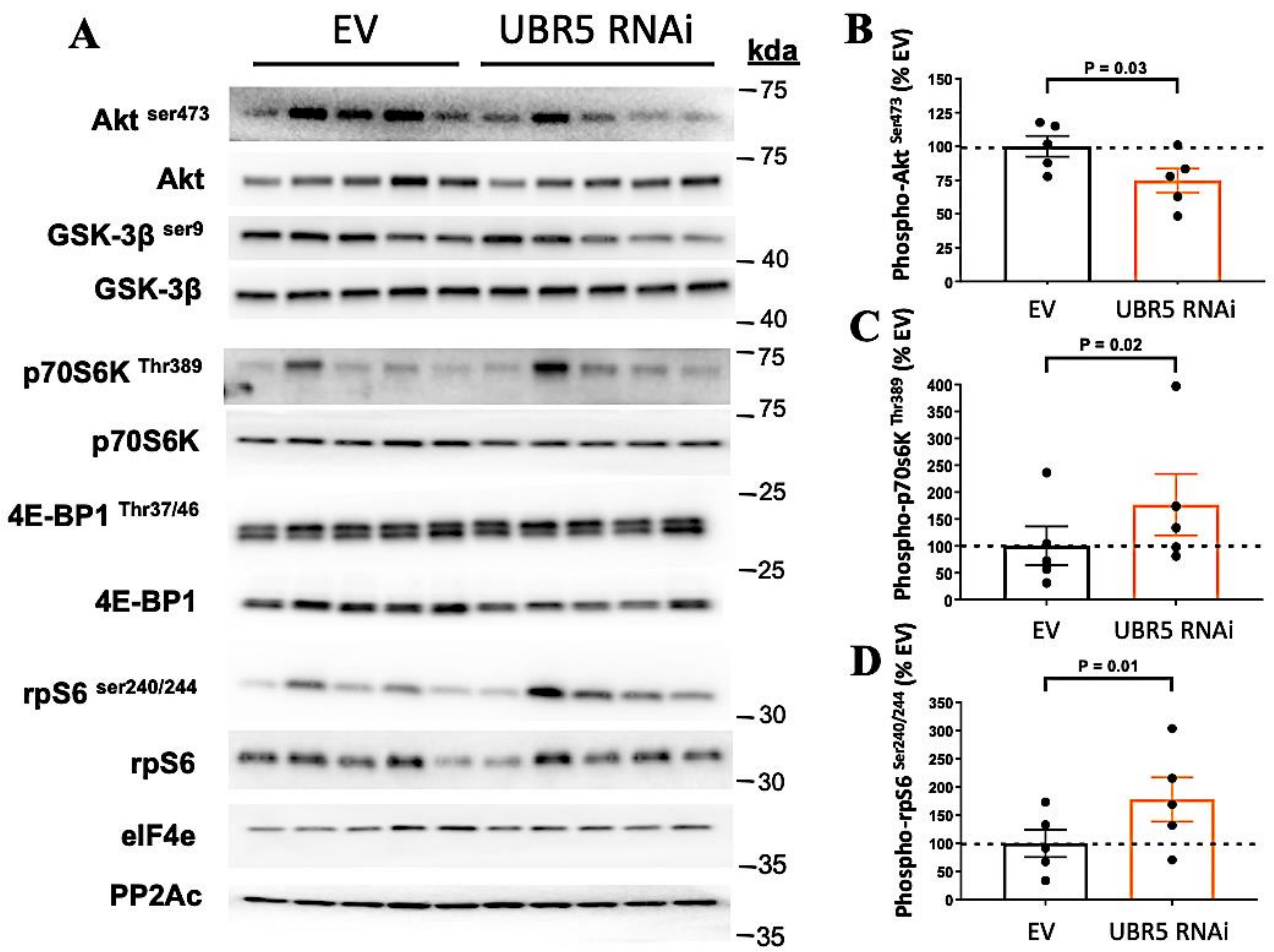

Figure 4. (A) Western blot analysis for the Akt signaling pathway (Akt, GSK-3β, p70S6K, 4E-BP1, rpS6, eIF4e, PP2Ac) in UBR5 RNAi transfected TA muscle after 7 days. (B) Decreased phosphorylation levels of Akt (*P* = 0.03) and **(C)** increased phosphorylation levels of p70S6K and **(D)** rps6 with UBR5 RNAi. No significant changes in phosphorylation of GSK-3β, 4E-BP1 or total levels of eiF4e and PP2Ac were observed in UBR5 RNAi conditions at 7 days. All *n* = 5 per group – EV control and UBR5 RNAi. Data presented as Mean ± SEM. Total protein loading of the membranes captured from images using stain-free gel technology was used as the normalization control for all blots. Statistical significance is depicted where present (P ≥ 0.05).

Prolonged UBR5 RNAi transfection leads to significant loss of muscle mass and fiber CSA atrophy in mouse skeletal muscle

Given the data over 7 days, the next question to interrogate was the impact of UBR5 RNAi transfection in TA muscle after a prolonged period (30 days), with the hypothesis that this would perhaps lead to greater muscle atrophy vs. 7 days of UBR5 suppression. In line with this hypothesis, while UBR5 protein reductions were not maintained out to this 30-day timepoint (Figure 5A), the earlier reductions in UBR5 at 7 days led to a significant reduction in muscle mass by 30 days (-4.6 ± 1.5%) in UBR5 RNAi transfected vs. EV muscles (P = 0.01; Figure 5B). Alongside the reduction in

403 muscle mass, a significant larger reduction in GFP-positive fiber CSA (-18.2 ± 2.3% at 30 d vs. -9.5 ±
404 3.2% at 7 d) was evident after UBR5 RNAi transfection (*P* = 0.01; Figure 5C & D) vs. EV control, with
405 the RNAi transfected muscles displaying a shift in the distribution of fiber CSA primarily towards
406 smaller fibers (≥ 2600 μm^2) compared to the EV control muscle (Figure 5E). These observations
407 provide further support towards UBR5 being a positive modulator of muscle mass, with its
408 knockdown evoking considerable atrophy.
409

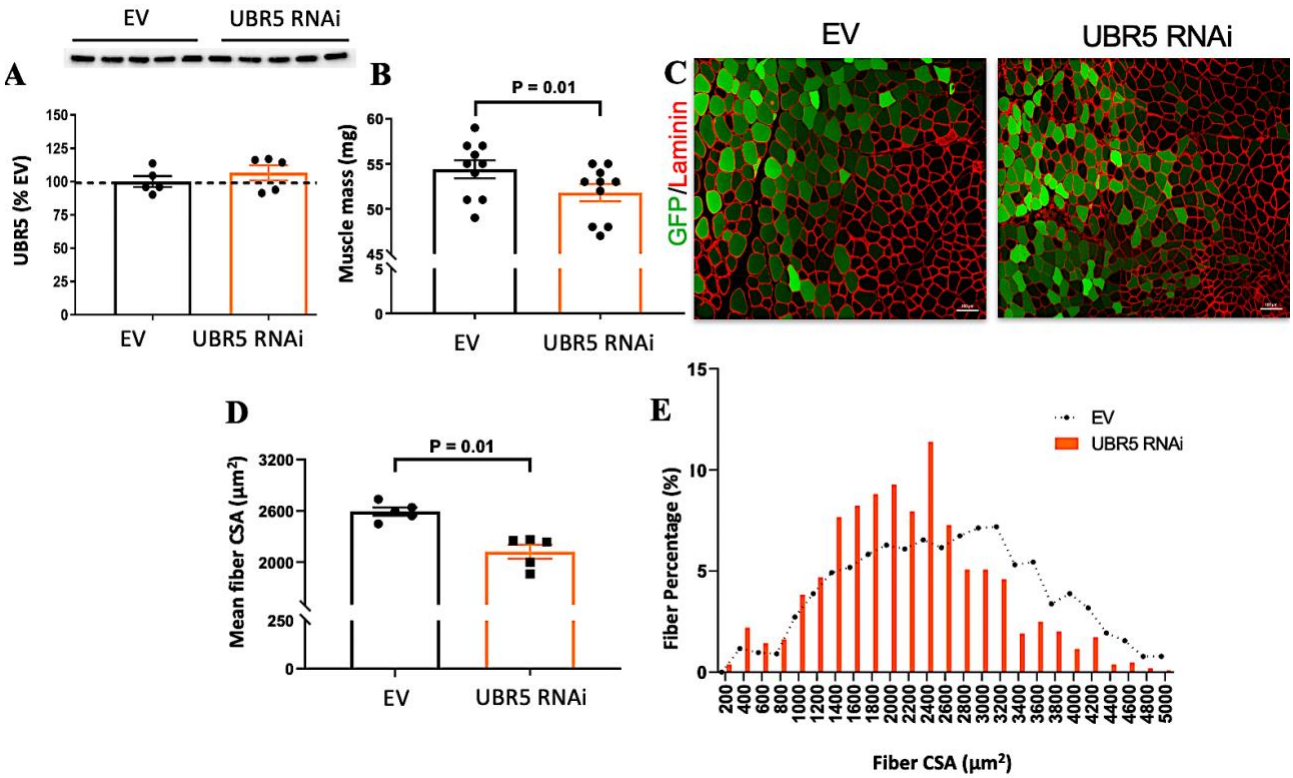

410
411 **Figure 5. Loss of muscle mass and fiber CSA in UBR5 RNAi transfected TA muscle after 30 days. (A)** UBR5 protein after
412 30 d UBR5 RNAi. (**B)** After 30 days, muscle mass was significantly reduced in UBR5 RNAi transfected vs. empty vector
413 control (EV) TA muscles (P = 0.01; *n* = 10 per group). **(C)** Representative images (10x magnification; scale bar = 100 μm)
414 for GFP transfected fiber identification and CSA quantification through Laminin staining. **(D)** A significant reduction (*P* =
415 0.01) in mean transfected fiber CSA size was observed in the RNAi transfected vs. EV muscles *(n* = 5 per group). **(E)**
416 Quantification of transfected muscle CSA revealed a leftward shift from large to smaller fiber sizes (≥3400 μm^2) with
417 RNAi transfected muscles verses EV group (**D**). Data presented as Mean ± SEM.
418
419 *Prolonged UBR5 RNAi at 30 days and reductions in muscle mass and fiber size are associated with*
420 *increased PP2Ac, reduced eIF4e and inappropriate chronic elevation of p70S6K and rpS6*
421 At 30 days post RNAi transfection we continued to observe an elevation in p90RSK phosphorylation,
422 similar to the 7d time point (Figure 6A). Opposite to the 7d time point, we observe significant
423 increases total p90RSK (Figure 6B) and both phosphorylated and total ERK (Figure 6C & 6D) in RNAi

transfected muscles after 30 days. As with 7 days we observed no differences in the phosphorylation of MEK 1/2$^{Ser\ 217/221}$ or MSK-1^{Thr581} between RNAi and EV transfected TA muscles after 30 days (data not depicted). By 30 days there was no reduction of phosphorylated Akt as observed at the 7-day timepoint and no change in GSK-3β phosphorylation with RNAi transfection (Figure 7A). Interestingly, elevation of p70S6K and rpS6 phosphorylation from the 7-day time point continued over the more chronic period of 30 days, demonstrating a 4- and 2-fold increase respectively in the RNAi transfected muscles verses the empty vector control group (Figure 7B & 7C). Compared to the 7d time point, we also observed an 80% reduction in eIF4e protein levels in the RNAi group (Figure 7D). Furthermore, the levels of PP2Ac were significantly increased at the 30 d time point (Figure 7E). Finally, like at 7 days there were no changes in activity of 4E-BP1 $^{Thr37/46}$ or its total levels in UBR5 RNAi transfected muscles at 30 days. Signalling events at 7 and 30 days are summarised in cell signalling diagram (Figure 8).

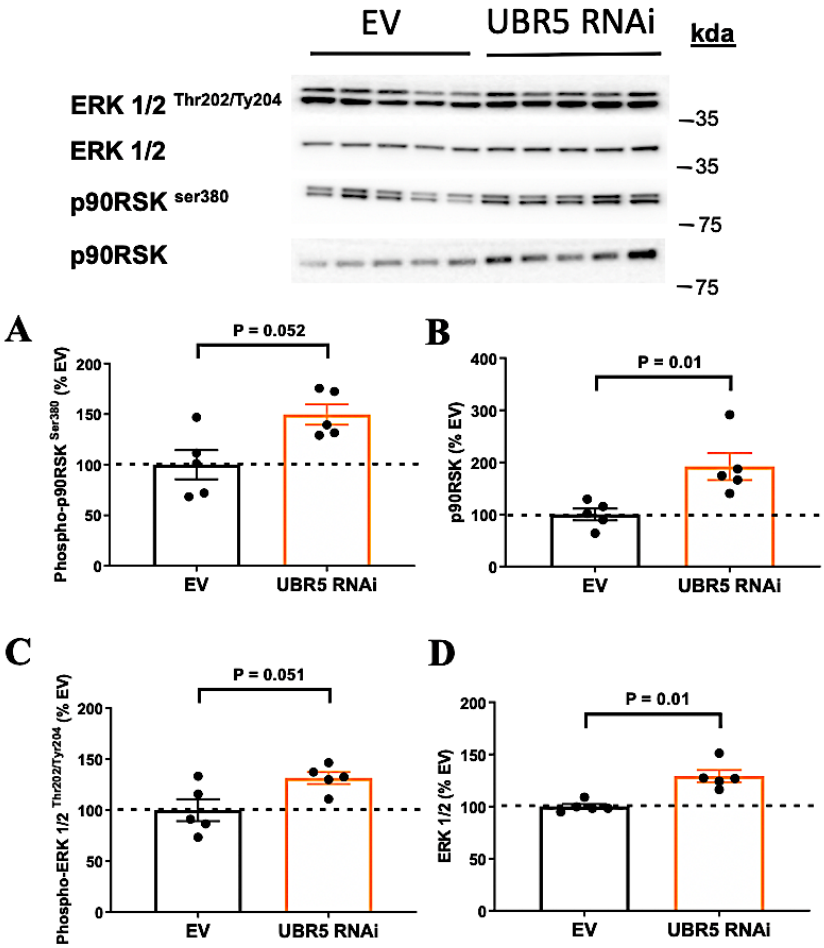

Figure 6. ERK pathways signaling in UBR5 RNAi transfected TA muscle after 30 days. (A) Phosphorylated p90RSK, **(B)** total p90RSK, **(C)** Phosphorylated ERK1/2 and **(D)** Total ERK. All *n* = 5 per group – EV control and UBR5 RNAi. Data presented as Mean ± SEM. Total protein loading of the membranes captured from images using stain-free gel technology was used as the normalization control for all blots. Statistical significance is depicted where present (P ≥ 0.05).

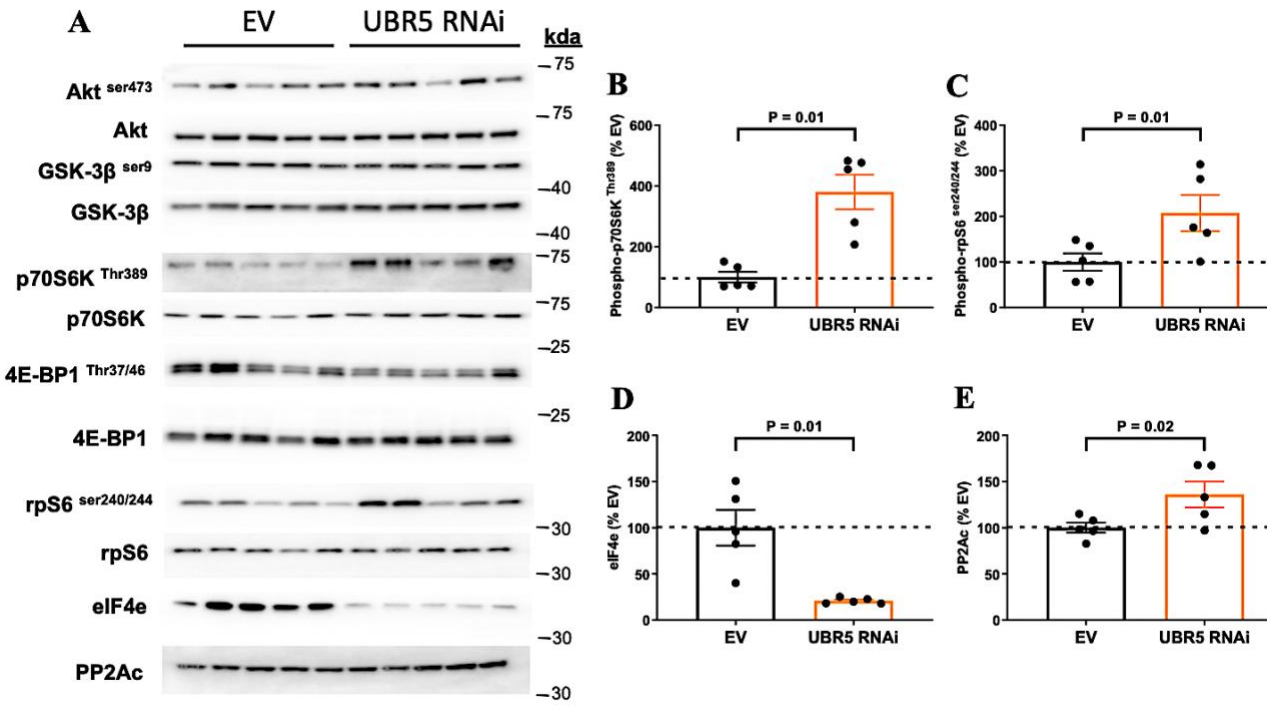

Figure 7. A) Western blot analysis for the Akt signaling pathway (Akt, GSK-3β, p70S6K, 4E-BP1, rpS6, eIF4e, PP2Ac) in UBR5 RNAi transfected TA muscle after 30 days. Significant changes observed for **(B)** Phosphorylated p70S6K, **(C)** Phosphorylated rpS6, **(D)** eIF4e and, **(E)** PP2Ac. All *n* = 5 per group – EV control and UBR5 RNAi. Data presented as Mean ± SEM. Total protein loading of the membranes captured from images using stain-free gel technology was used as the normalization control for all blots. Statistical significance is depicted where present (P ≥ 0.05).

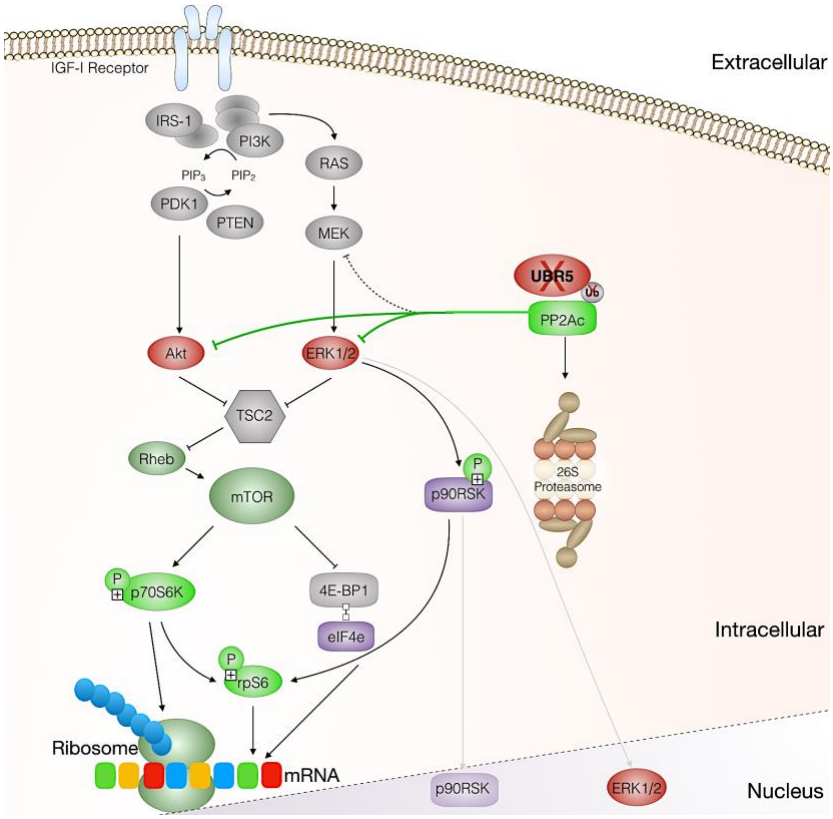

Figure 8. Schematic of cell signaling events after UBR5 knockdown in skeletal muscle in-vivo. UBR5 knockdown (X) increases phosphatase PP2Ac, reduces ERK and Akt phosphorylation (RED), reduces total p90RSK and eIF4e (PURPLE), chronically increases the phosphorylation of p70S6K and rpS6 (GREEN).

452 **Discussion**

453 The present study aimed to: 1) silence UBR5 in human myotubes using siRNA during mechanical
454 loading to confirm whether UBR5 was regulated in response to mechanical loading. Given
455 ERK/p90RSK and Akt/P70S6K signalling has been associated with load-induced anabolism,
456 ERK/p90RSK is altered with UBR5 manipulation in non-muscle cells, and PP2Ac is a negative
457 regulator of ERK and Akt that can be degraded by UBR5, we also aimed to: 2) investigate the impact
458 of reduced UBR5 on ERK and Akt signalling pathways in SkM tissue using our miR-based RNAi for
459 UBR5 electroporated into the tibialis anterior (TA) of mice.

460

461 We hereby report that mechanical loading of non-treated myotubes induced anincrease in UBR5
462 gene expression which was similar to that following acute loading in murine bioengineered SkM (35)
463 and acute RE in humans (36, 37). Furthermore, mechanical loading was able to prevent the siRNA-
464 induced reduction in UBR5 gene expression, which suggested that UBR5 gene expression may be
465 regulated via mechano-sensitive signalling. Indeed, transfection of UBR5 RNAi into the TA muscle of
466 mice after 7 days caused a significant reduction in fiber CSA, total RNA, global protein synthesis and
467 ERK1/2 / Akt phosphorylation. However, p90RSK, P70S6K and rps6 phosphorylation significantly
468 increased, perhaps suggestive of a potential compensatory mechanism triggered by the reduction
469 in UBR5 or inappropriate chronic activation of these pathways, like that observed in aged muscle
470 (discussed below). Furthermore, the increases in p90RSK phosphorylation were on a background of
471 considerably reduced total p90RSK levels. Finally, changes at 7 days also culminated in significant
472 reductions in muscle mass and an even greater reduction in fiber CSA after prolonged (30 days)
473 UBR5 RNAi. This was associated with increased PP2Ac and, as hypothesised above, continued
474 chronic elevation of P70S6K and rpS6 from 7 to 30 days, as well as reductions in elongation initiation
475 factor 4e (eIF4e). Overall, the present study further supports the notion that UBR5 plays an
476 important role in muscle anabolism and hypertrophy, and its reduction culminates in atrophy.

477

478 In the present study, transfection of UBR5 targeting siRNAs induced a ~77% reduction in UBR5
479 mRNA expression in non-loaded human myotubes. Following confirmation of effective UBR5
480 knockdown in non-loaded myotubes, UBR5 gene expression was assessed in response to mechanical
481 loading. Mechanical loading of non-treated myotubes displayed an increase (~158% / 1.58-fold) in
482 UBR5 gene expression (see Figure 1G), which was similar to the fold changes observed after an acute
483 bout of RE in human SkM (~1.71-fold) (Seaborne *et al.*, 2018*b*, 2018*a*) and the same fold changes
484 observed after acute loading in bioengineered SkM (~1.58-fold) (35). Significant changes in UBR5

485 gene expression were also achieved following chronic (7 weeks) training, and in retraining for which
486 greatest increase in UBR5 gene expression was observed (36, 37). Also, UBR5 significantly increased
487 after hypertrophy following 4 weeks of resistance training via programmed chronic high-frequency
488 electrical stimulation in rats (34, 35). Furthermore, we have previously reported a significant
489 increase in UBR5 following acute loading in bioengineered C_2C_{12} SkM (35). Finally, mechanical
490 loading was able to prevent the siRNA-induced reduction in UBR5 gene expression. Such a finding
491 perhaps suggested that UBR5 may be involved in mechano-sensitive signalling pathways.
492
493 Therefore, we next performed UBR5-specific knockdown experiments in mouse TA muscle, to
494 investigate the impact of reduced UBR5 on mechanical-induced signalling networks, ERK
495 (MEK/ERK/p90RSK/MSK1) and Akt (PP2Ac/Akt/GSK3β/P70S6K/4E-BP1/rpS6) pathways *in-vivo*.
496 Electroporation of UBR5 RNAi for 7 days induced a significant reduction in average myofiber CSA,
497 frequency of larger myofibers (≥3400 μm^2), total RNA and muscle protein synthesis (~17%) which
498 coincided with a reduction in ERK1/2 signalling. The reduction in total RNA and muscle protein
499 synthesis is interesting given the classification of UBR5 as an E3 ubiquitin ligase and thus its role in
500 the ubiquitin-proteasome system. Indeed, UBR5 may have unidentified functions within skeletal
501 muscle that are unrelated to proteasomal degradation. An example of an E3 ubiquitin ligase having
502 other functions in skeletal muscle is TRIM72 (known as MG53), with its role being studied in cell
503 membrane repair (6, 11, 12). UBR5 has been suggested to have a role in the regulation of mRNA
504 translation and gene regulation through the MLLE domain on the UBR5 protein structure (30, 44).
505 Recent studies have identified the translation capacity and activity of skeletal muscle to be
506 important for growth and hypertrophy in rodent and human models (20, 31, 39, 42). Therefore,
507 while we saw reductions in ERK/ Akt activity in the present study, there were opposite increases in
508 p90RSK, p70S6K and rps6 suggesting that the observed reductions in protein synthesis may not be
509 regulated by p90RSK, p70S6K and rps6 activity. However, there were significant reductions in total
510 p90RSK as a consequence of UBR5 knockdown at 7d, that may contribute to the reductions in
511 protein synthesis observed. However, given the observed reduction in total RNA, there could be a
512 role for UBR5 in the regulation of mRNA translational capacity that would in-turn lead to reductions
513 in total protein synthesis and SkM mass. Indeed, supporting this notion, we also observed 80%
514 reductions of eiF4e at 30 days, an elongation initiation factor important for enhanced RNA
515 translational efficiency, splicing and stability.
516

517 Other explanations for increased p90RSK, p70S6K and rpS6 signalling activity significantly increasing
518 following UBR5 knockdown, are perhaps due to a compensatory or protective mechanism in an
519 attempt to prevent the reductions in protein synthesis. Further, in a non-classically envisaged
520 pathway, the increase in p90RSK activity may be explained due to its suggested role as an upstream
521 regulator of UBR5 and its activation could therefore be altered due to the suppression of UBR5
522 protein levels (9). This could suggest that loss of UBR5 may indirectly lead to activation of p90RSK
523 because its normal target for action is no longer present. Alongside the alterations in p90RSK
524 phosphorylation, as suggested above, we did observe a significant loss in total protein levels for
525 p90RSK at 7 days which may contribute towards the alterations in p90RSK activity and the overall
526 reductions in protein synthesis. There are currently no commercial antibodies to assess UBR5
527 activity in relation to p90RSK, something that warrants investigation when antibodies are developed
528 in the future. In addition to alterations in ERK and Akt signalling and reduced total p90RSK and
529 protein synthesis at 7 days, a prolonged time period after transfection of the UBR5 RNAi at 30 days
530 resulted in greater reductions in both muscle mass and fiber CSA. The loss of muscle mass and fiber
531 size at 30 days, was surprisingly accompanied by increased p70S6K and rpS6 phosphorylation. The
532 chronic activation of mTORC/P70S6K signalling has been observed to be detrimental in skeletal
533 muscle homeostasis, such as that with increasing age (2, 8, 24, 38). Therefore, subsequent future
534 studies will seek to address the interplay between UBR5 and Akt/mTORC/p70S6K signalling with
535 aging.
536
537 Finally, in the present study we observed significant increases in PP2Ac levels at 30 d RNAi. PP2Ac
538 is a phosphatase demonstrated to inhibit Akt and ERK signalling, and importantly, UBR5 in its
539 capacity as an ubiquitin ligase has been demonstrated to target PP2A for degradation in non-muscle
540 studies (25–27, 38). While observing an increase in PP2Ac at 30 days, the reductions in signalling of
541 Akt and ERK were observed at 7 days and not at 30 days. However, the data does suggest for the
542 first time in skeletal muscle, that PP2A is perhaps a target of UBR5 and that knockdown of UBR5
543 leads to an increase in the levels of PP2A due to a potential decrease in its degradation. However,
544 UBR5 and its protein targets remain to be elucidated in skeletal muscle and require further study
545 given these interesting findings.
546
547 Despite the exciting and novel findings surrounding UBR5's mechanistic role in skeletal muscle, it is
548 worth acknowledging the limitations of the study. Firstly, neither puromycin incorporation nor
549 subsequent measures of total protein synthesis were assessed in human myotubes. This was due to

550 the limited human cellular material available during experimentation. It was therefore not feasible
551 to extract protein for all conditions, nor to examine cellular signalling in siUBR5 treated vs. non-
552 treated human myotubes. However, we subsequently performed this signalling analysis *in-vivo*. It is
553 also important to note that UBR5 protein levels were not reduced at 30 d to the same degree as the
554 7d time point and this may be reflective of the effectiveness of the RNAi construct being reduced
555 and also the influence of non-transfected muscle fibers in the biochemical analyses. However, the
556 earlier reductions in UBR5 at 7 days still evoked altered signalling and greatest loss of muscle mass
557 by this 30-day timepoint. Suggesting the earlier reductions in UBR5 at 7 days still culminated in later
558 atrophy by 30 days. Lastly, it would also be prudent in future experiments to also evoke hypertrophy
559 (e.g. via synergistic ablation) in rodents in the presence or absence of the UBR5 RNAi plasmid.
560
561 **Conclusion**
562 The present study supports the notion that UBR5 plays an important role in muscle
563 anabolism/hypertrophy, and presents novel findings demonstrating knockdown of UBR5 is
564 associated with early reductions in ERK1/2 and Akt activity, total p90RSK and protein synthesis that
565 culminates in later atrophy that is associated with increased PP2Ac, reduced eIF4e levels and
566 inappropriately chronically elevated activity of p70S6K and rpS6.
567
568
569 **Author contributions**
570 DCT, DCH, LMB, SCB, APS conceived and designed the research. All authors were involved in
571 acquisition or analysis or interpretation of data for the work. DCT, DCH, LMB, SCB, APS drafted the
572 work. All Authors were involved in revising the work critically for important intellectual content. All
573 authors approved the final version of the manuscript.
574
575 **Funding**
576 DCT was funded via PhD studentships from Keele University and Liverpool John Moores University
577 (LJMU) via APS. DCTs project was further supported by the Society for Endocrinology equipment
578 grant and the North Staffordshire Medical Institute awarded to APS. RAS was funded by Doctoral
579 Alliance/ LJMU funded PhD studentship via APS and further supported by grants awarded to APS
580 from GlaxoSmithKline. PG was funded by EPSRC/MRC (UKRI) PhD studentship via APS and Keele
581 University doctoral training centre and is now supported by the Norwegian School of Sport Sciences.
582 DCH & LMB was supported by the University of Iowa in the laboratory of SCB.

583

584 **Declarations & Competing Interests**

585 SCB is on the scientific advisory board for Emmyon Inc. The authors declare that they have no other
586 competing interests.

587

588 **Data Availability Statement**

589 The data that support the findings of this study are available from the corresponding author upon
590 reasonable request.

591

592 **Acknowledgments**

593 We wish to thank Dr. David S. Waddell (University of North Florida) and Mr. George R. Marcotte
594 (University of Iowa) for technical assistance with the project.

595

596 **References**

597 1. **Baar K**, **Torgan CE**, **Kraus WE**, **Esser K**. Autocrine Phosphorylation of p70 S6k in Response to
598 Acute Stretch in Myotubes. *Mol Cell Biol Res Commun* 4: 76–80, 2000.

599 2. **Bentzinger CF**, **Lin S**, **Romanino K**, **Castets P**, **Guridi M**, **Summermatter S**, **Handschin C**,
600 **Tintignac LA**, **Hall MN**, **Rüegg MA**. Differential response of skeletal muscles to mTORC1
601 signaling during atrophy and hypertrophy. *Skelet Muscle* 3: 1–16, 2013.

602 3. **Bodine SC**, **Baehr LM**. Skeletal muscle atrophy and the E3 ubiquitin ligases MuRF1 and
603 MAFbx/atrogin-1. *Am J Physiol - Endocrinol Metab* 307: E469–E484, 2014.

604 4. **Bodine SC**, **Latres E**, **Baumhueter S**, **Lai VKM**, **Nunez L**, **Clarke BA**, **Poueymirou WT**, **Panaro**
605 **FJ**, **Erqian Na**, **Dharmarajan K**, **Pan ZQ**, **Valenzuela DM**, **Dechiara TM**, **Stitt TN**, **Yancopoulos**
606 **GD**, **Glass DJ**. Identification of ubiquitin ligases required for skeletal Muscle Atrophy. *Science*
607 *(80-)* 294: 1704–1708, 2001.

608 5. **Bodine SC**, **Stitt TN**, **Gonzalez M**, **Kline WO**, **Stover GL**, **Bauerlein R**, **Zlotchenko E**,
609 **Scrimgeour A**, **Lawrence JC**, **Glass DJ**, **Yancopoulos GD**. Akt/mTOR pathway is a crucial
610 regulator of skeletal muscle hypertrophy and can prevent muscle atrophy in vivo. *Nat Cell*

611 *Biol* 3: 1014–1019, 2001.

612 6. **Cai C**, **Masumiya H**, **Weisleder N**, **Matsuda N**, **Nishi M**, **Hwang M**, **Ko J**, **Lin P**, **Thornton A**,
613 **Zhao X**, **Pan Z**, **Komazaki S**, **Brotto M**, **Takeshima H**, **Ma J**. MG53 nucleates assembly of cell
614 membrane repair machinery Chuanxi. *Nat Cell Biol* 11: 56–64, 2009.

615 7. **Cao PR**, **Kim HJ**, **Lecker SH**. Ubiquitin-protein ligases in muscle wasting. *Int J Biochem Cell*
616 *Biol* 37: 2088–2097, 2005.

617 8. **Castets P**, **Lin S**, **Rion N**, **Fulvio S Di**, **Romanino K**, **Guridi M**, **Frank S**, **Tintignac LA**, **Sinnreich**
618 **M**, **Ruegg MA**. Sustained Activation of mTORC1 in Skeletal Muscle Inhibits Constitutive and
619 Starvation-Induced Autophagy and Causes a Severe, Late-Onset Myopathy. *Cell Metab* 17:
620 731–744, 2013.

621 9. **Cho JH**, **Kim SA**, **Seo YS**, **Park SG**, **Park BC**, **Kim JH**, **Kim S**. The p90 ribosomal S6 kinase–
622 UBR5 pathway controls Toll-like receptor signaling via miRNA-induced translational
623 inhibition of tumor necrosis factor receptor–associated factor 3. *J Biol Chem* 292: 11804–
624 11814, 2017.

625 10. **Crown A**, **He X**, **Holly J**, **Lightman S**, **Stewart C**. Characterisation of the IGF system in a
626 primary adult human skeletal muscle cell model, and comparison of the effects of insulin
627 and IGF-I on protein metabolism. *J Endocrinol* 167: 403–415, 2000.

628 11. **Demonbreun AR**, **McNally EM**. Plasma Membrane Repair in Health and Disease. *Curr Top*
629 *Membr* 77: 67–96, 2016.

630 12. **Demonbreun AR**, **Quattrocelli M**, **Barefield DY**, **Allen M V.**, **Swanson KE**, **McNally EM**. An
631 actin-dependent annexin complex mediates plasma membrane repair in muscle. *J Cell Biol*
632 213: 705–718, 2016.

633 13. **Drummond MJ**, **Fry CS**, **Glynn EL**, **Dreyer HC**, **Dhanani S**, **Timmerman KL**, **Volpi E**,
634 **Rasmussen BB**. Rapamycin administration in humans blocks the contraction-induced
635 increase in skeletal muscle protein synthesis. *J Physiol* 587: 1535–1546, 2009.

636 14. **Ebert SM**, **Dyle MC**, **Kunkel SD**, **Bullard SA**, **Bongers KS**, **Fox DK**, **Dierdorff JM**, **Foster ED**,
637 **Adams CM**. Stress-induced skeletal muscle Gadd45a expression reprograms myonuclei and
638 causes muscle atrophy. *J Biol Chem* 287: 27290–27301, 2012.
639 15. **Eblen ST**, **Kumar NV**, **Shah K**, **Henderson MJ**, **Watts CKW**, **Shokat KM**, **Weber MJ**.
640 Identification of novel ERK2 substrates through use of an engineered kinase and ATP
641 analogs. *J Biol Chem* 278: 14926–14935, 2003.
642 16. **Goldberg A**. Work-induced growth of skeletal muscle in normal and hypophysectomized
643 rats. *Am J Physiol* 213: 1193–8, 1967.
644 17. **Gomes MD**, **Lecker SH**, **Jagoe RT**, **Navon A**, **Goldberg AL**. Atrogin-1, A Muscle-Specific F-Box
645 Protein Highly Expressed during Muscle Atrophy Author(s): *PNAS* 98: 14440–14445, 2001.
646 18. **Goodman CA**, **Frey JW**, **Mabrey DM**, **Jacobs BL**, **Lincoln HC**, **You JS**, **Hornberger TA**. The role
647 of skeletal muscle mTOR in the regulation of mechanical load-induced growth. *J Physiol* 589:
648 5485–5501, 2011.
649 19. **Goodman CA**, **Mabrey DM**, **Frey JW**, **Miu MH**, **Schmidt EK**, **Pierre P**, **Hornberger TA**. Novel
650 insights into the regulation of skeletal muscle protein synthesis as revealed by a new
651 nonradioactive in vivo technique . *FASEB J* 25: 1028–1039, 2011.
652 20. **Hammarström D**, **Øfsteng S**, **Koll L**, **Hanestadhaugen M**, **Hollan I**, **Apró W**, **Whist JE**,
653 **Blomstrand E**, **Rønnestad BR**, **Ellefsen S**. Benefits of higher resistance-training volume are
654 related to ribosome biogenesis. *J Physiol* 598: 543–565, 2020.
655 21. **Hornberger TA**, **Armstrong DD**, **Koh TJ**, **Burkholder TJ**, **Esser KA**. Intracellular signaling
656 specificity in response to uniaxial vs . multiaxial stretch : implications for
657 mechanotransduction. *Am J Physiol Physiol* 288: C185–C194, 2005.
658 22. **Hughes DC**, **Baehr LM**, **Discroll JR**, **Lynch SA**, **Waddell DS**, **Bodine SC**. Identification and
659 Characterization of Fbxl22, a novel skeletal muscle atrophy-promoting E3 ubiquitin ligase.
660 *Am. J. Physiol. - Cell Physiol.* (2020). doi: 10.1152/ajpcell.00253.2020.

661 23. **Hunt LC**, **Stover J**, **Haugen B**, **Shaw TI**, **Li Y**, **Pagala VR**, **Finkelstein D**, **Barton ER**, **Fan Y**,
662 **Labelle M**, **Peng J**, **Demontis F**. A Key Role for the Ubiquitin Ligase UBR4 in Myofiber
663 Hypertrophy in Drosophila and Mice. *Cell Rep* 28: 1268–1281, 2019.
664 24. **Joseph GA**, **Wang SX**, **Jacobs CE**, **Zhou W**, **Kimble GC**, **Tse HW**, **Eash JK**, **Shavlakadze T**, **Glass**
665 **DJ**. Partial Inhibition of mTORC1 in Aged Rats Counteracts the Decline in Muscle Mass and
666 Reverses Molecular Signaling Associated with Sarcopenia. *Mol Cell Biol* 39: 1–16, 2019.
667 25. **Labuzan SA**, **Lynch SA**, **Cooper LM**, **Waddell DS**. Inhibition of protein phosphatase
668 methylesterase 1 dysregulates MAP kinase signaling and attenuates muscle cell
669 differentiation. *Gene* 739: 1–14, 2020.
670 26. **Macdonald TM**, **Thomas LN**, **Daze E**, **Marignani P**, **Barnes PJ**, **Too CK**. Prolactin-inducible
671 EDD E3 ubiquitin ligase promotes TORC1 signalling , anti-apoptotic protein expression , and
672 drug resistance in breast cancer cells. *Am J Cancer Res* 9: 1484–1503, 2019.
673 27. **Mcdonald WJ**, **Sangster SM**, **Moffat LD**, **Henderson MJ**, **Too CKL**. a4 Phosphoprotein
674 Interacts With EDD E3 Ubiquitin Ligase and Poly(A)-Binding Protein. *J Cell Biochem* 110:
675 1123–1129, 2010.
676 28. **Miyazaki M**, **Mccarthy JJ**, **Fedele MJ**, **Esser KA**. Early activation of mTORC1 signalling in
677 response to mechanical overload is independent of phosphoinositide 3-kinase/Akt
678 signalling. *J Physiol* 589: 1831–1846, 2011.
679 29. **Moore DR**, **Atherton PJ**, **Rennie MJ**, **Tarnopolsky MA**, **Phillips SM**. Resistance exercise
680 enhances mTOR and MAPK signalling in human muscle over that seen at rest after bolus
681 protein ingestion. *Acta Physiol* 201: 365–372, 2011.
682 30. **Muńoz-Escobar J**, **Matta-Camacho E**, **Kozlov G**, **Gehring K**. The MLLE domain of the
683 ubiquitin ligase UBR5 binds to its catalytic domain to regulate substrate binding. *J Biol Chem*
684 290: 22841–22850, 2015.
685 31. **Nakada S**, **Ogasawara R**, **Kawada S**, **Maekawa T**, **Ishii N**. Correlation between ribosome

686 biogenesis and the magnitude of hypertrophy in overloaded skeletal muscle. *PLoS One* 11:
687 1–14, 2016.
688 32. **Owens DJ**, **Sharples AP**, **Polydorou I**, **Alwan N**, **Donovan T**, **Tang J**, **Fraser WD**, **Cooper RG**,
689 **Morton JP**, **Stewart C**, **Close GL**. A systems-based investigation into vitamin D and skeletal
690 muscle repair, regeneration, and hypertrophy. *Am J Physiol - Endocrinol Metab* 309: E1019–
691 E1031, 2015.
692 33. **Schmittgen TD**, **Livak KJ**. Analyzing real-time PCR data by the comparative CT method. *Nat*
693 *Protoc* 3: 1101–1108, 2008.
694 34. **Schmoll M**, **Unger E**, **Sutherland H**, **Haller M**, **Bijak M**, **Lanmuller H**, **Jarvis JC**. SpillOver
695 stimulation : A novel hypertrophy model using co-contraction of the plantar- flexors to load
696 the tibial anterior muscle in rats. *PLoS One* 13: 1–19, 2018.
697 35. **Seaborne R.**, **Hughes DC**, **Turner DC**, **Owens DJ**, **Baehr LM**, **Gorski P**, **Semenova EA**, **Borisov**
698 **O V.**, **Larin AK**, **Popov D V.**, **Generozov E V.**, **Sutherland H**, **Ahmetov II**, **Jarvis JC**, **Bodine SC**,
699 **Sharples AP**. UBR5 is a novel E3 ubiquitin ligase involved in skeletal muscle hypertrophy and
700 recovery from atrophy. *J Physiol* 597: 3727–3749, 2019.
701 36. **Seaborne R.**, **Strauss J**, **Cocks M**, **Shepherd S**, **O'Brien T.**, **van Someren K.**, **Bell P.**,
702 **Murgatroyd C**, **Morton J.**, **Stewart C.**, **Mein C.**, **Sharples A.** Data Descriptor : Methylome of
703 human skeletal muscle after acute & chronic resistance exercise training , detraining &
704 retraining. *Sci Data* 5: 1–9, 2018.
705 37. **Seaborne R.**, **Strauss J**, **Cocks M**, **Shepherd S**, **O'Brien T.**, **Van Someren K.**, **Bell P.**,
706 **Murgatroyd C**, **Morton J.**, **Stewart C.**, **Sharples A.** Human Skeletal Muscle Possesses an
707 Epigenetic Memory of Hypertrophy. *Sci Rep* 8: 1–17, 2018.
708 38. **Seshacharyulu P**, **Pandey P**, **Datta K**, **Batra SK**. Phosphatase : PP2A structural importance ,
709 regulation and its aberrant expression in cancer. *Cancer Lett* 335: 9–18, 2013.
710 39. **Stec MJ**, **Kelly NA**, **Many GM**, **Windham ST**, **Tuggle SC**, **Bamman MM**. Ribosome biogenesis

711 may augment resistance training-induced myofiber hypertrophy and is required for
712 myotube growth in vitro. *Am J Physiol - Endocrinol Metab* 310: E652–E661, 2016.
713 40. **Turner DC**, **Kasper AM**, **Seaborne RA**, **Brown AD**, **Close GL**, **Murphy M**, **Stewart CE**, **Martin**
714 **NRW**, **Sharples AP**. Exercising Bioengineered Skeletal Muscle In Vitro: Biopsy to Bioreactor.
715 In: *Methods in Molecular Biology*, edited by Rønning S. New York, NY: Springer International
716 Publishing, 2019, p. 55–79.
717 41. **Wen Y**, **Murach KA**, **Vechetti IJ**, **Fry CS**, **Vickery C**, **Peterson CA**, **McCarthy JJ**, **Campbell KS**.
718 Myo Vision: Software for automated high-content analysis of skeletal muscle
719 immunohistochemistry. *J Appl Physiol* 124: 40–51, 2018.
720 42. **West DWD**, **Baehr LM**, **Marcotte GR**, **Chason CM**, **Tolento L**, **Gomes A V.**, **Bodine SC**, **Baar**
721 **K**. Acute resistance exercise activates rapamycin-sensitive and -insensitive mechanisms that
722 control translational activity and capacity in skeletal muscle. *J Physiol* 594: 453–468, 2016.
723 43. **Williamson D**, **Gallagher P**, **Harber M**, **Hollon C**, **Trappe S**. Mitogen-activated protein kinase
724 (MAPK) pathway activation: Effects of age and acute exercise on human skeletal muscle. *J*
725 *Physiol* 547: 977–987, 2003.
726 44. **Xie J**, **Kozlov G**, **Gehring K**. The “tale” of poly(A) binding protein: The MLLE domain and
727 PAM2-containing proteins. *Biochim Biophys Acta - Gene Regul Mech* 1839: 1062–1068,
728 2014.
729 45. **Yu M**, **Blomstrand E**, **Chibalin A V.**, **Krook A**, **Zierath JR**. Marathon running increases ERK1/2
730 and p38 MAP kinase signalling to downstream targets in human skeletal muscle. *J Physiol*
731 536: 273–282, 2001.
732